

MAGNETIC FIELD INTEGRAL EQUATION FOR ELECTROMAGNETIC SCATTERING BY CONDUCTING BODIES OF REVOLUTION IN LAYERED MEDIA

A. A. K. Mohsen and A. K. Abdelmageed

Engineering Mathematics and Physics Department
Cairo University
Giza 12211, Egypt

- 1. Introduction**
 - 2. Problem Statement**
 - 3. Development of the MFIE-BOR Formulation**
 - 4. Application to the Contiguous Half-Spaces**
 - 4.1 Modal Sommerfeld Integrals
 - 4.2 MSIs Evaluation Using DCIM
 - 5. Numerical Results**
 - 6. Conclusion**
- References**

1. INTRODUCTION

Electromagnetic scattering by objects in layered media is one of the topics that have received great interest due to its vast applications in radar detection, remote sensing, geophysical exploration and communication. Abdelmageed et al. [1] have developed recently an electric field integral equation for conducting bodies of revolution (EFIE-BOR) in layered media. The EFIE is an integral equation of the first kind which is suitable for both open and closed objects. Based on the magnetic field integral equation, a new formulation for conducting BOR in layered media (MFIE-BOR) is presented. MFIE is an integral equation of the second kind. This makes MFIE have better stability and conditioning than EFIE particularity for large objects. Although MFIE is not suitable for open surfaces; however it finds its greatest use for

large closed surfaces [2]. This property is of great importance for the analysis of objects in layered media. In this case, the CPU time for generating the equivalent matrix of EFIE/MFIE is multiples of its corresponding free space case. This means that the saving in CPU time using MFIE is more pronounced in layered medium compared with free space. This makes MFIE more advantageous than EFIE for the electromagnetic analysis of closed objects in layered media.

The MFIE-BOR formulation is expressed in terms of Sommerfeld integrals (SIs). One of the efficient techniques to tackle these integrals is the discrete complex image method (DCIM). The idea of the method was initiated by the first author in [3] and developed numerically by Fang et al. [4]. This method is adopted here. In this technique, the integrand of the SI is transformed via the pencil-of-function method (POFM) [5] into a short series of complex exponentials. Using Sommerfeld identities, the resulting integrals are transformed into closed-form solutions of similar form as the free space solution. This makes the formulation very efficient from both the implementation and computation points of view.

The paper is organized as follows. In section 2, the problem of a conducting BOR in layered media is stated. In section 3, the MFIE-BOR formulation is developed. The application of DCIM to the SIs present in the MFIE-BOR formulation is introduced in section 4. In section 5 sample results are given to solidate our formulation. The summary and some concluding remarks are included in section 6.

2. PROBLEM STATEMENT

Consider the BOR illustrated in Fig. 1, where it is formed by rotating a planar curve, called the “generating arc”, around the Z -axis which is the axis of the BOR. The ℓ -coordinate follows the generating arc on the body surface S . The BOR is immersed in a layered medium, and illuminated by an incident plane wave. The material layers are homogeneous and of infinite extent along the X and Y axes. The top and bottom layers may be of infinite extent along Z -axis, as shown in the figure. The n th layer is characterized by a relative permittivity ϵ_n and a relative permeability μ_n . The free space permittivity and permeability are denoted by ϵ_o and μ_o , respectively.

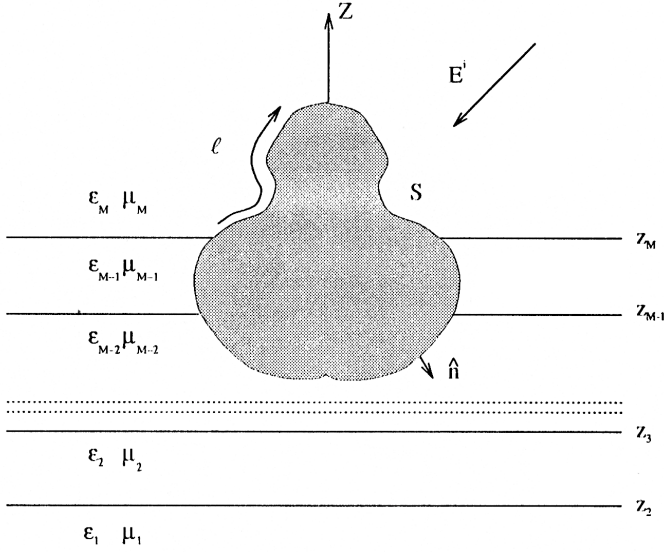


Figure 1. A body of revolution in layered medium.

3. DEVELOPMENT OF THE MFIE-BOR FORMULATION

According to the equivalence theorem [6], the original problem of Fig. 1 may be replaced by its equivalent where the conducting object is removed and its effect replaced by as yet unknown electric surface current density \mathbf{K} , residing on a mathematical surface S . The magnetic field \mathbf{H} may be represented in terms of the vector Green's function $\underline{\underline{\mathbf{G}}}^A$ in the form

$$\mathbf{H}(\mathbf{r}) = \mathbf{H}^i(\mathbf{r}) + \frac{1}{j\omega\mu} \nabla \times \int dS' \underline{\underline{\mathbf{G}}}^A(\mathbf{r}|\mathbf{r}') \cdot \mathbf{K}(\mathbf{r}') \quad (1)$$

where \mathbf{H}^i is the incident magnetic field. The time variation $e^{j\omega t}$ has been assumed and suppressed. Application of the boundary conditions on the surface S yields

$$\hat{\mathbf{n}} \times \mathbf{H}^i(\mathbf{r}) = \frac{1}{2} \mathbf{K}(\mathbf{r}) - \frac{1}{j\omega\mu} \hat{\mathbf{n}} \times \nabla \times \int dS' \underline{\underline{\mathbf{G}}}^A(\mathbf{r}|\mathbf{r}') \cdot \mathbf{K}(\mathbf{r}') \quad (2)$$

where $\hat{\mathbf{n}}$ is the outward unit normal vector. Eq. (2) is the MFIE which is an integral equation of the second kind in \mathbf{K} ; while EFIE is an integral equation of the first kind. This form of MFIE is suited

for closed smooth surfaces; while EFIE is suitable for both open and closed surfaces [2]. The smoothness condition restricts the application of the MFIE. However, the formulation can be generalized for all closed objects. This is possible if we account for the field behavior at the parts of the surface where the boundary is not locally plane. At these parts, MFIE given by (2) should be corrected as [2].

$$\hat{\mathbf{n}} \times \mathbf{H}^i(\mathbf{r}) = \left(1 - \frac{\Omega}{4\pi}\right) \mathbf{K}(\mathbf{r}) - \frac{1}{j\omega\mu} \hat{\mathbf{n}} \times \nabla \times \int dS' \underline{\underline{\mathbf{G}}}^A(\mathbf{r}|\mathbf{r}') \cdot \mathbf{K}(\mathbf{r}') \quad (3)$$

where Ω is the solid angle subtended by the surface at the concerned part. When this part is locally plane, $\Omega = 2\pi$ and the factor $(1 - \frac{\Omega}{4\pi})$ becomes $\frac{1}{2}$ which is the same as in (2). For large closed bodies, MFIE finds its greatest use since the geometrical factor $(1 - \frac{\Omega}{4\pi}) \mathbf{K}$ often tends to make the contribution from the integral of only second-order importance [2].

The form of $\underline{\underline{\mathbf{G}}}^A$ of a conducting body in a layered medium is not unique. Michalski and Zheng [7, 8] have developed three distinct forms. We will be concerned here with the so-called ‘‘Formulation C’’. For this formulation, Michalski and Zheng [7] obtained for z in layer j and z' in layer n

$$\begin{aligned} \underline{\underline{\mathbf{G}}}^A(\boldsymbol{\rho} - \boldsymbol{\rho}'; z|z') = & \underline{\underline{\mathbf{I}}}_t S_o \left\{ V_i^h \right\} \\ & - (\hat{\mathbf{z}}\hat{\mathbf{x}} \cos \vartheta + \hat{\mathbf{z}}\hat{\mathbf{y}} \sin \vartheta) j k_o \eta_o \mu_j S_1 \left\{ \frac{I_i^h - I_i^e}{k_\rho^2} \right\} \\ & - (\hat{\mathbf{x}}\hat{\mathbf{z}} \cos \vartheta + \hat{\mathbf{y}}\hat{\mathbf{z}} \sin \vartheta) j k_o \eta_o \mu_n S_1 \left\{ \frac{V_v^h - V_v^e}{k_\rho^2} \right\} \\ & + \hat{\mathbf{z}}\hat{\mathbf{z}} \eta_o^2 \frac{\mu_n}{\epsilon_j} S_o \left\{ I_v^e + \frac{k_j^2}{k_\rho^2} \left(I_v^h - \frac{k_{zn}^2}{k_n^2} I_v^e \right) \right\} \end{aligned} \quad (4)$$

where

$$S_\nu\{\cdot\} = \frac{1}{2\pi} \int_0^\infty dk_\rho k_\rho^{\nu+1} J_\nu(k_\rho |\boldsymbol{\rho} - \boldsymbol{\rho}'|) \{\cdot\}; \quad \nu = 0, 1 \quad (5)$$

$$\vartheta = \arctan \left\{ \frac{y - y'}{x - x'} \right\}, \quad k_{zn} = \sqrt{k_n^2 - k_\rho^2} \quad (6)$$

J_ν is the Bessel function of order ν . $\underline{\underline{\mathbf{I}}}_t$ is the unit dyadic transverse to z , and $k_n = k_o \sqrt{\mu_n \epsilon_n}$ is the wavenumber of the n th layer.

The spectral functions V_v^p , I_v^p , V_i^p , I_i^p are the transmission line (TL) Green's functions, where p denotes either e (TM) or h (TE). The argument $(k_\rho; z|z')$ of these spectral functions is omitted for notational simplicity.

At the surface of the BOR, (3) may be split into the following coupled equations

$$H_\varphi^i = \left(1 - \frac{\Omega}{4\pi}\right) K_\ell - \frac{1}{j\omega\mu} \hat{\ell} \cdot \hat{\mathbf{n}} \times \nabla \times \int dS' \underline{\underline{\mathbf{G}}}^A(\mathbf{r}|\mathbf{r}') \cdot \mathbf{K}(\mathbf{r}') \quad (7)$$

$$H_\ell^i = - \left(1 - \frac{\Omega}{4\pi}\right) K_\varphi + \frac{1}{j\omega\mu} \hat{\varphi} \cdot \hat{\mathbf{n}} \times \nabla \times \int dS' \underline{\underline{\mathbf{G}}}^A(\mathbf{r}|\mathbf{r}') \cdot \mathbf{K}(\mathbf{r}') \quad (8)$$

where K_ℓ and K_φ are the current components in the $\hat{\ell}$ and $\hat{\varphi}$ directions, respectively, and

$$\hat{\mathbf{n}} = \cos \gamma \cos \varphi \hat{\mathbf{x}} + \cos \gamma \sin \varphi \hat{\mathbf{y}} - \sin \gamma \hat{\mathbf{z}} \quad (9)$$

$$\hat{\varphi} = -\sin \varphi \hat{\mathbf{x}} + \cos \varphi \hat{\mathbf{y}} \quad (10)$$

$$\hat{\ell} = \sin \gamma \cos \varphi \hat{\mathbf{x}} + \sin \gamma \sin \varphi \hat{\mathbf{y}} + \cos \gamma \hat{\mathbf{z}} \quad (11)$$

γ is the angle between the tangent to the generating curve, $\hat{\ell}$, and the Z -axis, defined to be positive if $\hat{\ell}$ points away from the Z -axis and negative if $\hat{\ell}$ points toward the Z -axis. To take advantage of the rotational symmetry in the problem, the currents, incident fields and SIs are expanded in Fourier series in φ . Hence, $\mathbf{H}^i(\mathbf{r})$ and $\mathbf{K}(\mathbf{r})$ are expanded in the form

$$\mathbf{H}^i(\mathbf{r}) = \sum_{m=-\infty}^{\infty} \left[H_\ell^{im}(\ell) \hat{\ell} + H_\varphi^{im}(\ell) \hat{\varphi} \right] e^{jm\varphi} \quad (12)$$

$$\mathbf{K}(\mathbf{r}) = \sum_{m=-\infty}^{\infty} \left[K_\ell^m(\ell) \hat{\ell} + K_\varphi^m(\ell) \hat{\varphi} \right] e^{jm\varphi} \quad (13)$$

where $K_\ell^m(H_\ell^{im})$ and $K_\varphi^m(H_\varphi^{im})$ represent the modal current density (incident field) components in the $\hat{\ell}$ and $\hat{\varphi}$ directions, respectively. Since the formulation involves derivatives with respect to ξ where $\xi = \rho, \varphi, z$, we will adopt here different expansions to that used in deriving the EFIE-BOR. For $S_o\{f\}$, where f is a spectral function of argument $(k_\rho; z|z')$, we expand its derivative as

$$\frac{\partial S_o\{f\}}{\partial \xi} = \sum_{m=-\infty}^{\infty} f_\xi^m e^{jm(\varphi-\varphi')}; \quad \xi = \rho, \varphi, z \quad (14)$$

where

$$f_{\xi}^m = \frac{1}{4\pi^2} \int_{-\pi}^{\pi} d(\varphi - \varphi') e^{-jm(\varphi - \varphi')} \frac{\partial}{\partial \xi} \int_0^{\infty} dk_{\rho} k_{\rho} f(k_{\rho}; z|z') J_0(k_{\rho}|\boldsymbol{\rho} - \boldsymbol{\rho}'|) \quad (15)$$

while $S_1\{f\}$ is expanded using Graf's theorem [9] as

$$\begin{aligned} \frac{\cos}{\sin}(\varphi - \vartheta) S_1\{f\} &= \pm \frac{1}{2\pi} \frac{\cos}{\sin}(\psi) \int_0^{\infty} dk_{\rho} k_{\rho}^2 f(k_{\rho}; z|z') J_1(k_{\rho}|\boldsymbol{\rho} - \boldsymbol{\rho}'|) \\ &= \pm \frac{1}{2\pi} \int_0^{\infty} dk_{\rho} k_{\rho}^2 \frac{f^c}{f_s}(k_{\rho}; z|z') e^{-j\psi} \\ &\quad \cdot \sum_{m=-\infty}^{\infty} J_{m+1}(k_{\rho}\rho) J_m(k_{\rho}\rho') e^{jm(\varphi - \varphi')} \\ &= \pm \sum_{m=-\infty}^{\infty} \frac{f^{cm}}{f^{sm}}(\rho, \rho'; z|z') e^{jm(\varphi - \varphi')} \end{aligned} \quad (16)$$

where

$$\frac{f^c}{f_s}(k_{\rho}; z|z') = \frac{\cos}{\sin}(\psi) f(k_{\rho}; z|z') \quad (17)$$

$$\frac{f^{cm}}{f^{sm}}(\rho, \rho'; z|z') = \frac{1}{2\pi} \int_0^{\infty} dk_{\rho} k_{\rho}^2 \frac{f^c}{f_s}(k_{\rho}; z|z') e^{-j\psi} J_{m+1}(k_{\rho}\rho) J_m(k_{\rho}\rho') \quad (18)$$

and for its derivative, we use

$$\frac{\partial}{\partial \xi} \left\{ \frac{\cos}{\sin}(\varphi - \vartheta) S_1\{f\} \right\} = \sum_{m=-\infty}^{\infty} \frac{f_{\xi}^{cm}}{f_{\xi}^{sm}} e^{jm(\varphi - \varphi')} \quad (19)$$

where

$$\begin{aligned} \frac{f_{\xi}^{cm}}{f_{\xi}^{sm}} &= \pm \frac{1}{4\pi^2} \int_{-\pi}^{\pi} d(\varphi - \varphi') e^{-jm(\varphi - \varphi')} \\ &\quad \cdot \frac{\partial}{\partial \xi} \int_0^{\infty} dk_{\rho} k_{\rho}^2 \frac{f^c}{f_s}(k_{\rho}; z|z') J_1(k_{\rho}|\boldsymbol{\rho} - \boldsymbol{\rho}'|) \end{aligned} \quad (20)$$

The angle ψ is depicted in Fig. 2, and it is given by

$$\psi = \tan^{-1} \frac{\rho' \sin \beta}{\rho - \rho' \cos \beta}; \quad \beta = \phi - \phi' \quad (21)$$

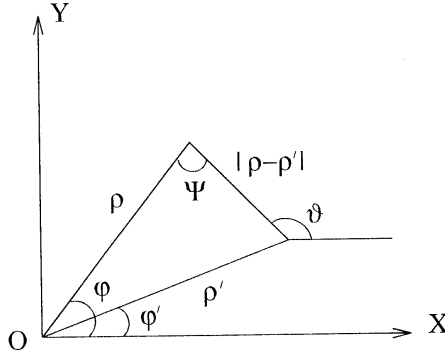


Figure 2. Coordinates of the source and field points.

In view of (12)–(20) and after lengthy algebraic manipulation, the MFIE equations (7) and (8) take the form

$$\begin{aligned}
 H_{\varphi}^{im} = & \left(1 - \frac{\Omega}{4\pi}\right) K_{\ell}^m - \frac{\pi}{\omega\mu} \int d\ell' \rho' K_{\varphi}^m(\ell') \left(L_{(tt)z}^{m+1} - L_{(tt)z}^{m-1}\right) \\
 & - \frac{\pi}{j\omega\mu} \int d\ell' \rho' K_{\ell}^m(\ell') \left[\sin \gamma' \left(L_{(tt)z}^{m+1} + L_{(tt)z}^{m-1}\right) - 2 \cos \gamma' L_{(zz)\rho}^m\right] \\
 & + \frac{2\pi}{j\omega\mu} \int d\ell' \rho' K_{\ell}^m(\ell') \cos \gamma' L_{(tz)z}^{cm} \\
 & - \frac{\pi}{j\omega\mu} \int d\ell' \rho' K_{\ell}^m(\ell') \sin \gamma' \\
 & \cdot \left[\left(L_{(zt)\rho}^{c(m+1)} + L_{(zt)\rho}^{c(m-1)}\right) - j \left(L_{(zt)\rho}^{s(m+1)} - L_{(zt)\rho}^{s(m-1)}\right)\right] \\
 & - \frac{\pi}{j\omega\mu} \int d\ell' \rho' K_{\ell}^m(\ell') \\
 & \cdot \left[j \left(L_{(zt)\rho}^{c(m+1)} - L_{(zt)\rho}^{c(m-1)}\right) + \left(L_{(zt)\rho}^{s(m+1)} + L_{(zt)\rho}^{s(m-1)}\right)\right] \quad (22)
 \end{aligned}$$

$$\begin{aligned}
 H_{\ell}^{im} = & -\left(1 - \frac{\Omega}{4\pi}\right) K_{\varphi}^m + \frac{\pi}{j\omega\mu} \int d\ell' \rho' K_{\varphi}^m(\ell') \sin \gamma \left(L_{(tt)z}^{m+1} + L_{(tt)z}^{m-1}\right) \\
 & - \frac{\pi}{j\omega\mu} \int d\ell' \rho' K_{\ell}^m(\ell') \\
 & \cdot \left[\frac{2}{\rho} \sin \gamma \cos \gamma' L_{(zz)\varphi}^m + j \sin \gamma \sin \gamma' \left(L_{(tt)z}^{m+1} - L_{(tt)z}^{m-1}\right)\right] \\
 & + \frac{\pi}{j\rho\omega\mu} \int d\ell' \rho' K_{\ell}^m(\ell') \cos \gamma \sin \gamma'
 \end{aligned}$$

$$\begin{aligned}
& \cdot \left[j\rho \left(L_{(tt)\rho}^{m+1} - L_{(tt)\rho}^{m-1} \right) + \left(L_{(tt)\varphi}^{m+1} + L_{(tt)\varphi}^{m-1} \right) \right] \\
& - \frac{\pi}{j\rho\omega\mu} \int d\ell' \rho' K_{\varphi}^m(\ell') \cos \gamma \\
& \cdot \left[\rho \left(L_{(tt)\rho}^{m+1} + L_{(tt)\rho}^{m-1} \right) - j \left(L_{(tt)\varphi}^{m+1} - L_{(tt)\varphi}^{m-1} \right) \right] \\
& + \frac{\pi}{j\rho\omega\mu} \int d\ell' \rho' K_{\ell}^m(\ell') \sin \gamma \sin \gamma' \\
& \cdot \left[\left(L_{(zt)\varphi}^{c(m+1)} + L_{(zt)\varphi}^{c(m-1)} \right) - j \left(L_{(zt)\varphi}^{s(m+1)} - L_{(zt)\varphi}^{s(m-1)} \right) \right] \\
& + \frac{\pi}{j\rho\omega\mu} \int d\ell' \rho' K_{\varphi}^m(\ell') \sin \gamma \\
& \cdot \left[j \left(L_{(zt)\varphi}^{c(m+1)} - L_{(zt)\varphi}^{c(m-1)} \right) + \left(L_{(zt)\varphi}^{s(m+1)} + L_{(zt)\varphi}^{s(m-1)} \right) \right] \\
& - \frac{\pi}{j\rho\omega\mu} \int d\ell' \rho' K_{\ell}^m(\ell') \sin \gamma \sin \gamma' \\
& \cdot \left[j \left(L_{zt}^{c(m+1)} - L_{zt}^{c(m-1)} \right) + \left(L_{zt}^{s(m+1)} + L_{zt}^{s(m-1)} \right) \right] \\
& + \frac{\pi}{j\rho\omega\mu} \int d\ell' \rho' K_{\varphi}^m(\ell') \sin \gamma \\
& \cdot \left[\left(L_{zt}^{c(m+1)} + L_{zt}^{c(m-1)} \right) - j \left(L_{zt}^{s(m+1)} - L_{zt}^{s(m-1)} \right) \right] \\
& - \frac{2\pi}{j\omega\mu} \int d\ell' \rho' K_{\ell}^m(\ell') \sin \gamma \cos \gamma' L_{(tz)z}^{sm} \\
& + \frac{2\pi}{j\rho\omega\mu} \int d\ell' \rho' K_{\ell}^m(\ell') \cos \gamma \cos \gamma' \left[L_{tz}^{sm} + \rho L_{(zt)\rho}^{sm} - L_{(zt)\varphi}^{cm} \right] \quad (23)
\end{aligned}$$

The equations are given in terms of the spatial derivatives of the modal Sommerfeld integrals (MSIs) $L_{(tt)\xi}^m$, $L_{(zz)\xi}^m$, $L_{(zt)\xi}^m$, $L_{(tz)\xi}^m$ and L_{zt}^m , L_{tz}^m which are expressed as

$$L_{(tt)\xi}^m = \mathcal{T}_{m0}^{\xi} \left\{ k_{zn} V_i^h \right\} \quad (24)$$

$$L_{(zz)\xi}^m = \frac{\eta_{o2}^2 \mu_2}{\epsilon_n} \mathcal{T}_{m0}^{\xi} \left\{ k_{zn} I_v^e + k_{zn} \frac{k_n^2}{k_{\rho}^2} \left(I_v^h - \frac{k_{zj}^2}{k_j^2} I_v^e \right) \right\} \quad (25)$$

$$\frac{L_{zt}^{cm}}{L_{zt}^{sm}} = \pm j \eta_o k_o \mu_n \mathcal{T}_{m1} \left\{ \operatorname{sgn}(z) \frac{\cos}{\sin}(\psi) e^{-j\psi} \frac{k_{zn}}{k_{\rho}^2} \left(I_i^h - I_i^e \right) \right\} \quad (26)$$

$$\frac{L_{tz}^{cm}}{L_{tz}^{sm}} = \pm j \eta_o k_o \mu_n \mathcal{T}_{m1} \left\{ \frac{\cos}{\sin}(\psi) e^{-j\psi} \frac{k_{zn}}{k_{\rho}^2} \left(V_v^h - V_v^e \right) \right\} \quad (27)$$

$$\frac{L_{(zt)\xi}^{cm}}{L_{(zt)\xi}^{sm}} = \pm j\eta_o k_o \mu_n \mathcal{T}_{m1}^{\xi} \left\{ \frac{\cos(\psi)}{\sin(\psi)} \frac{k_{zn}}{k_{\rho}^2} \left(I_i^h - I_i^e \right) \right\} \quad (28)$$

$$\frac{L_{(tz)\xi}^{cm}}{L_{(tz)\xi}^{sm}} = \pm j\eta_o k_o \mu_j \mathcal{T}_{m1}^{\xi} \left\{ \frac{\cos(\psi)}{\sin(\psi)} \frac{k_{zn}}{k_{\rho}^2} \left(V_v^h - V_v^e \right) \right\} \quad (29)$$

where

$$\begin{aligned} \mathcal{T}_{m\nu}^{\xi}\{\cdot\} &= \frac{1}{4\pi^2} \int_{-\pi}^{\pi} d(\varphi - \varphi') e^{-jm(\varphi - \varphi')} \\ &\quad \cdot \frac{\partial}{\partial \xi} \int_0^{\infty} dk_{\rho} \frac{k_{\rho}^{\nu+1}}{k_{zn}} J_{\nu}(k_{\rho}|\boldsymbol{\rho} - \boldsymbol{\rho}'|)\{\cdot\} \end{aligned} \quad (30)$$

$$\mathcal{T}_{m\nu}\{\cdot\} = \frac{1}{2\pi} \int_0^{\infty} dk_{\rho} \frac{k_{\rho}^{\nu+1}}{k_{zn}} J_{m+\nu}(k_{\rho}\rho) J_m(k_{\rho}\rho')\{\cdot\} \quad (31)$$

(22) and (23) constitute the MFIE-BOR which govern the current distribution on the surface of a conducting BOR embedded in a layered medium. The solution of these two coupled equations yields the modal currents K_{ℓ}^m and K_{φ}^m of mode m . In order to obtain the total currents K_{ℓ} and K_{φ} , as expressed by (13), we have to solve these equations on a mode-by-mode basis, with subsequent application of the superposition principle.

4. APPLICATION TO THE CONTIGUOUS HALF-SPACES

4.1 Modal Sommerfeld Integrals

For contiguous half-spaces, the TL Green's functions are given in [8]. Substituting for these functions we can deduce that for z and z' within the same n th layer, the MSIs can be expressed as

$$\begin{aligned} L_{(tt)\xi}^m &= \frac{k_o \eta_o \mu_n}{2} \\ &\quad \cdot \mathcal{T}_{m0}^{\xi} \left\{ e^{-jk_{zn}|z-z'|} + \overleftrightarrow{\Gamma}_q^h e^{-jk_{zn}|z+z'|} + \left[\overleftrightarrow{\Gamma}_q^h - \overleftrightarrow{\Gamma}_q^e \right] e^{-jk_{zn}|z+z'|} \right\} \end{aligned} \quad (32)$$

$$L_{(zz)\xi}^m = \frac{k_o \eta_o \mu_n}{2} \mathcal{T}_{m0}^{\xi} \left\{ e^{-jk_{zn}|z-z'|} + \left(\overleftrightarrow{\Gamma}_q^h - 2\overleftrightarrow{\Gamma}_q^e \right) e^{-jk_{zn}|z+z'|} \right\}$$

$$+ \left[-\overleftrightarrow{\Gamma}^e - \frac{k_{zn}^2}{k_\rho^2} \left(\overleftrightarrow{\Gamma}^h - \overleftrightarrow{\Gamma}^e \right) - \overleftrightarrow{\Gamma}_q^h + 2\overleftrightarrow{\Gamma}_q^e \right] e^{-jk_{zn}|z+z'|} \Big\} \quad (33)$$

$$\begin{aligned} \frac{L_{zt}^{cm}}{L_{zt}^{sm}} &= -\frac{L_{tz}^{cm}}{L_{tz}^{sm}} = \pm \frac{j\eta_o k_o \mu_n}{2} \\ &\cdot \mathcal{T}_{m1} \left\{ \left[sgn(z) \frac{\cos(\psi)}{\sin(\psi)} e^{-j\psi} \frac{k_{zn}}{k_\rho^2} \left(\overleftrightarrow{\Gamma}^h - \overleftrightarrow{\Gamma}^e \right) \right] e^{-jk_{zn}|z+z'|} \right\} \end{aligned} \quad (34)$$

$$\begin{aligned} \frac{L_{(zt)\xi}^{cm}}{L_{(zt)\xi}^{sm}} &= -\frac{L_{(tz)\xi}^{cm}}{L_{(tz)\xi}^{sm}} \\ &= \pm \frac{j\eta_o k_o \mu_n}{2} \mathcal{T}_{m1}^\xi \left\{ \left[sgn(z) \frac{\cos(\psi)}{\sin(\psi)} \frac{k_{zn}}{k_\rho^2} \left(\overleftrightarrow{\Gamma}^h - \overleftrightarrow{\Gamma}^e \right) \right] e^{-jk_{zn}|z+z'|} \right\} \end{aligned} \quad (35)$$

and for z in layer j and z' in layer n

$$L_{(tt)\xi}^m = \frac{k_o \eta_o \mu_n}{2} \mathcal{T}_{m0}^\xi \left\{ \left[\overleftrightarrow{\mathcal{R}}^h e^{-jk_{zj}|z|} \right] e^{-jk_{zn}|z'|} \right\} \quad (36)$$

$$\begin{aligned} L_{(zz)\xi}^m &= \frac{k_o \eta_o \mu_n}{2} \mathcal{T}_{m0}^\xi \left\{ \left[-\overleftrightarrow{\mathcal{R}}^e e^{-jk_{zn}|z|} \right. \right. \\ &\quad \left. \left. - \frac{k_n^2}{k_\rho^2} \left(\frac{k_{zn}^2}{k_n^2} \overleftrightarrow{\mathcal{R}}^h - \frac{k_{zj}^2}{k_j^2} \overleftrightarrow{\mathcal{R}}^e \right) e^{-jk_{zj}|z|} \right] e^{-jk_{zn}|z'|} \right\} \end{aligned} \quad (37)$$

$$\begin{aligned} \frac{L_{zt}^{cm}}{L_{zt}^{sm}} &= -\frac{\mu_j}{\mu_n} \frac{L_{tz}^{cm}}{L_{tz}^{sm}} = \pm \frac{j\eta_o k_o \mu_j}{2} \\ &\cdot \mathcal{T}_{m1} \left\{ \left[sgn(z) \frac{\cos(\psi)}{\sin(\psi)} e^{-j\psi} \frac{k_{zn}}{k_\rho^2} \left(\overleftrightarrow{\Gamma}^h - \overleftrightarrow{\Gamma}^e \right) e^{-jk_{zj}|z|} \right] e^{-jk_{zn}|z'|} \right\} \end{aligned} \quad (38)$$

$$\begin{aligned} \frac{L_{(zt)\xi}^{cm}}{L_{(zt)\xi}^{sm}} &= -\frac{\mu_j}{\mu_n} \frac{L_{(tz)\xi}^{cm}}{L_{(tz)\xi}^{sm}} = \pm \frac{j\eta_o k_o \mu_j}{2} \\ &\cdot \mathcal{T}_{m1}^\xi \left\{ \left[sgn(z) \frac{\cos(\psi)}{\sin(\psi)} \frac{k_{zn}}{k_\rho^2} \left(\overleftrightarrow{\Gamma}^h - \overleftrightarrow{\Gamma}^e \right) e^{-jk_{zj}|z|} \right] e^{-jk_{zn}|z'|} \right\} \end{aligned} \quad (39)$$

$$\overleftrightarrow{\mathcal{R}}^p = 1 + \overleftrightarrow{\Gamma}^p \quad (40)$$

where $\overleftrightarrow{\Gamma}^p$ is the terminal reflection coefficient, and $\overleftrightarrow{\Gamma}_q^p$ is its corresponding value when $k_\rho \rightarrow \infty$. The lower (upper) arrow is used

for $z' \geq 0$ ($z' < 0$). In (32) and (33), both the homogeneous and quasi-static terms are extracted.

4.2 MSIs Evaluation Using DCIM

The MSIs of the MFIE-BOR for the case of contiguous half-spaces are given by (32)–(39). When the source and field points share the same layer and for $L_{(tt)\xi}^m$, $L_{(zz)\xi}^m$ the spectral function is split into three parts. The first and second parts represent the homogeneous and quasi-static terms, respectively. These terms can be resolved into closed-form solutions using the Sommerfeld identity [10]:

$$\frac{e^{-jk_n R}}{R} = -j \int_0^\infty dk_\rho k_\rho \frac{e^{-jk_{zn} z}}{k_{zn}} J_o(k_\rho |\boldsymbol{\rho} - \boldsymbol{\rho}'|) \quad (41)$$

where

$$R = \sqrt{|\boldsymbol{\rho} - \boldsymbol{\rho}'|^2 + z^2} \quad (42)$$

The third part (square-bracketed term) and the other MSIs have no apparent closed-form solution. However, the DCIM can be used efficiently to evaluate these integrals. The square-bracketed expressions are sampled and the complex images are extracted using POFM [5]. Doing this and in view of (41) and its derivative with respect to $|\boldsymbol{\rho} - \boldsymbol{\rho}'|$, then (32)–(39) reduce to

$$L_{(tt)\xi}^m = \frac{j\eta_o k_o \mu_n}{8\pi^2} \mathcal{S}_m^\xi \left\{ \frac{e^{-jk_n R}}{R} + \overleftrightarrow{\Gamma}_q^h \frac{e^{-jk_n R^q}}{R^q} + \sum_{l=1}^M A_l^{tt} \frac{e^{-jk_n R_l^{tt}}}{R_l^{tt}} \right\} \quad (43)$$

$$L_{(zz)\xi}^m = \frac{j\eta_o k_o \mu_n}{8\pi^2} \cdot \mathcal{S}_m^\xi \left\{ \frac{e^{-jk_n R}}{R} + \left(\overleftrightarrow{\Gamma}_q^h - 2\overleftrightarrow{\Gamma}_q^e \right) \frac{e^{-jk_n R^q}}{R^q} + \sum_{l=1}^M A_l^{zz} \frac{e^{-jk_n R_l^{zz}}}{R_l^{zz}} \right\} \quad (44)$$

$$\frac{L_{zt}^{cm}}{L_{zt}^{sm}} = -\frac{L_{tz}^{cm}}{L_{tz}^{sm}} = \pm \frac{jk_o \eta_o \mu_n}{8\pi^2} \cdot \mathcal{S}_m \left\{ \sum_{l=1}^M A_l^{zt} \frac{j|\boldsymbol{\rho} - \boldsymbol{\rho}'|}{R_l^{zt3}} [1 + jk_n R_l^{zt}] \frac{\cos(\psi)}{\sin} e^{-jk_n R_l^{zt}} \right\} \quad (45)$$

$$\begin{aligned} \frac{L_{(zt)\xi}^{cm}}{L_{(zt)\xi}^{sm}} &= -\frac{L_{(tz)\xi}^{cm}}{L_{(tz)\xi}^{sm}} = \pm \frac{jk_o\eta_o\mu_n}{8\pi^2} \\ &\cdot \mathcal{S}_m^\xi \left\{ \sum_{l=1}^M A_l^{zt} \frac{j|\boldsymbol{\rho} - \boldsymbol{\rho}'|}{R_l^{zt3}} [1 + jk_n R_l^{zt}] e^{j\psi \cos(\psi)} e^{-jk_n R_l^{zt}} \right\} \end{aligned} \quad (46)$$

where

$$\mathcal{S}_m\{\cdot\} = \int_{-\pi}^{\pi} d(\varphi - \varphi') e^{-jm(\varphi - \varphi')} \{\cdot\} \quad (47)$$

$$\mathcal{S}_m^\xi\{\cdot\} = \int_{-\pi}^{\pi} d(\varphi - \varphi') e^{-jm(\varphi - \varphi')} \frac{\partial}{\partial \xi} \{\cdot\} \quad (48)$$

$$R = \sqrt{|\boldsymbol{\rho} - \boldsymbol{\rho}'|^2 + (z - z')^2} \quad (49)$$

$$R^q = \sqrt{|\boldsymbol{\rho} - \boldsymbol{\rho}'|^2 + (z + z')^2} \quad (50)$$

$$R_l^\chi = \sqrt{|\boldsymbol{\rho} - \boldsymbol{\rho}'|^2 + (z + z' + \zeta_l^\chi)^2}; \quad \chi = tt, zz, zt, tz \quad (51)$$

for z and z' in the same n -layer. For z in layer j and z' in layer n , we have

$$L_{(tt)\xi}^m = \frac{j\eta_o k_o \mu_n}{8\pi^2} \mathcal{S}_m^\xi \left\{ \sum_{l=1}^M A_l^{tt} \frac{e^{-jk_n R_l^{tt}}}{R_l^{tt}} \right\} \quad (52)$$

$$L_{(zz)\xi}^m = \frac{j\eta_o k_o \mu_n}{8\pi^2} \mathcal{S}_m^\xi \left\{ \sum_{l=1}^M A_l^{zz} \frac{e^{-jk_n R_l^{zz}}}{R_l^{zz}} \right\} \quad (53)$$

$$\begin{aligned} \frac{L_{zt}^{cm}}{L_{zt}^{sm}} &= -\frac{\mu_j}{\mu_n} \frac{L_{tz}^{cm}}{L_{tz}^{sm}} = \pm \frac{jk_o\eta_o\mu_j}{8\pi^2} \\ &\cdot \mathcal{S}_m \left\{ \sum_{l=1}^M A_l^{zt} \frac{j|\boldsymbol{\rho} - \boldsymbol{\rho}'|}{R_l^{zt3}} [1 + jk_n R_l^{zt}] \frac{\cos(\psi)}{\sin(\psi)} e^{-jk_n R_l^{zt}} \right\} \end{aligned} \quad (54)$$

$$\begin{aligned} \frac{L_{(zt)\xi}^{cm}}{L_{(zt)\xi}^{sm}} &= -\frac{\mu_j}{\mu_n} \frac{L_{(tz)\xi}^{cm}}{L_{(tz)\xi}^{sm}} = \pm \frac{jk_o\eta_o\mu_j}{8\pi^2} \\ &\cdot \mathcal{S}_m^\xi \left\{ \sum_{l=1}^M A_l^{zt} \frac{j|\boldsymbol{\rho} - \boldsymbol{\rho}'|}{R_l^{zt3}} [1 + jk_n R_l^{zt}] \frac{\cos(\psi)}{\sin(\psi)} e^{j\psi} e^{-jk_n R_l^{zt}} \right\} \end{aligned} \quad (55)$$

$$R_l^x = \sqrt{|\boldsymbol{\rho} - \boldsymbol{\rho}'|^2 + (z' + \zeta_l^x)^2} \quad (56)$$

5. NUMERICAL RESULTS

The MFIE-BOR is solved using Glisson and Wilton approach for a BOR in free space [11]. The results of a conducting sphere of radius $a = 0.2\lambda_o$ in contiguous half-spaces are shown in Figs. 3, 4. The currents are plotted versus the normalized parameter s , which runs from $s = 0(\ell_o)$ to $s = 1(\ell_f)$, where (ℓ_o) and (ℓ_f) are the starting and ending tips of the generating arc ℓ . In Fig. 3, the sphere is half-buried with incident plane wave of $\theta^i = 60.0^\circ$. In Fig. 4, the sphere is buried with $\theta^i = 0.0^\circ$ and $d = -0.7\lambda_o$ where d is the vertical distance from the interface to the lower tip of the sphere. The $+$ ($-$) sign means that the lower tip is in the upper (lower) half-space. The results of both EFIE-BOR and MFIE-BOR are included where a good agreement is achieved.

For smooth objects, the singularity contribution term of the MFIE is $\frac{1}{2}$. As pointed out in Eq. (3), this term should be corrected to $(1 - \frac{\Omega}{4\pi})$ for non-smooth objects. To test the performance of MFIE-BOR in this case, results of a pillbox of radius $a = 0.159\lambda_o$, length $L = 1.0\lambda_o$ and $d = 0.1\lambda_o$ above ground are shown in Fig. 5. The plane wave is axially incident. At the corners of the pillbox, the surface subtends a solid angle $\Omega = \pi$. Therefore, all the segments of the generating arc have a singularity term equal to $\frac{1}{2}$ except for the segments that include a corner. In such case, the singularity term becomes $\frac{3}{4}$. As shown in Fig. 5, results of both EFIE-BOR and MFIE-BOR match well.

As stated in the introduction, MFIE-BOR is an integral equation of the second kind; while EFIE-BOR is an integral equation of the first kind. Hence, MFIE-BOR is more suitable for large closed bodies as this will be reflected on the convergence of the results. To make our point clear, we present three cases for a sphere in contiguous half-spaces of $\epsilon_1 = 10$ and $\epsilon_2 = 1$:

- Case I: A sphere in the upper space with $a = 1.0\lambda_o$ and $d = 0.2\lambda_o$.
- Case II: A sphere in the lower space with $a = 0.3\lambda_o$ and $d = -0.8\lambda_o$.
- Case III: A half-buried sphere with $a = 0.4\lambda_o$.

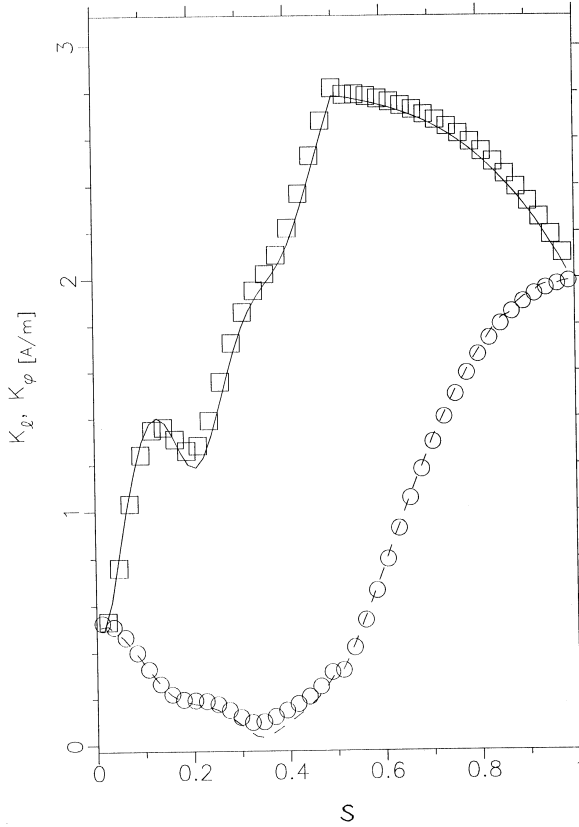


Figure 3. Magnitude of currents on a half-buried metallic sphere penetrating an air-earth interface with the parameters: $f = 0.3 \text{ GHz}$, $\epsilon_r = 15.0$, $\sigma = 0.025 \text{ [mho/m]}$, $\theta^i = 60.0^\circ$ and $a = 0.2\lambda_o$. EFIE-BOR: K_ℓ —, K_ϕ ---. MFIE-BOR: K_ℓ $\square\square\square$, K_ϕ $\circ\circ\circ$.

For brevity, the currents K_ℓ of case III are shown in Figs. 6, 7 for MFIE-BOR and EFIE-BOR, respectively. In each graph, the current is computed for different numbers of segments NS. Observing MFIE-BOR results, one can see that the results converge rapidly, and for NS = 31 good results can be obtained. For EFIE-BOR, results converge in a slower manner. For the first two cases, results begin to converge at NS = 41; while they converge at NS = 51 for the third case. In these examples, we used relatively fat spheres. This fortifies the claim that MFIE-BOR is more suitable for large closed objects.

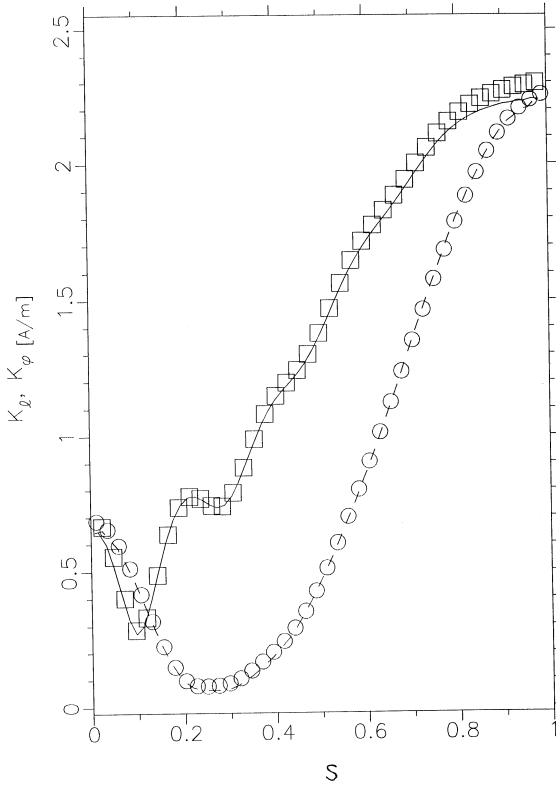


Figure 4. Magnitude of currents on a buried metallic sphere below an air-earth interface with the parameters: $f = 0.3$ GHz, $\epsilon_r = 15.0$, $\sigma = 0.025$ [mho/m], $\theta^i = 0.0^\circ$, $a = 0.2\lambda_o$ and $d = -0.7\lambda_o$. EFIE-BOR: K_ℓ —, K_φ - - -. MFIE-BOR: K_ℓ $\square\square\square$, K_φ $\circ\circ\circ$.

Table 1 shows the number of segments required for EFIE-BOR and MFIE-BOR to converge and their CPU times. The formulations have been implemented using Fortran Compiler on a 300-MHz Pentium. It is evident that MFIE-BOR is more efficient where a considerable saving in CPU time is obtained.

6. CONCLUSION

A MFIE-BOR formulation has been presented for conducting bodies of revolution in layered media with an application to the contiguous half-spaces. The discrete complex image method is used to evaluate

Formulation	No. of Segments NS			CPU Time		
	Case I	Case II	Case III	Case I	Case II	Case III
EFIE-BOR	41	41	51	32	42	90
MFIE-BOR	31	31	31	23	31	50

Table 1. The number of segments required for MFIE-BOR and EFIE-BOR of a sphere in contiguous half-spaces to converge and their corresponding CPU times (Sec.).

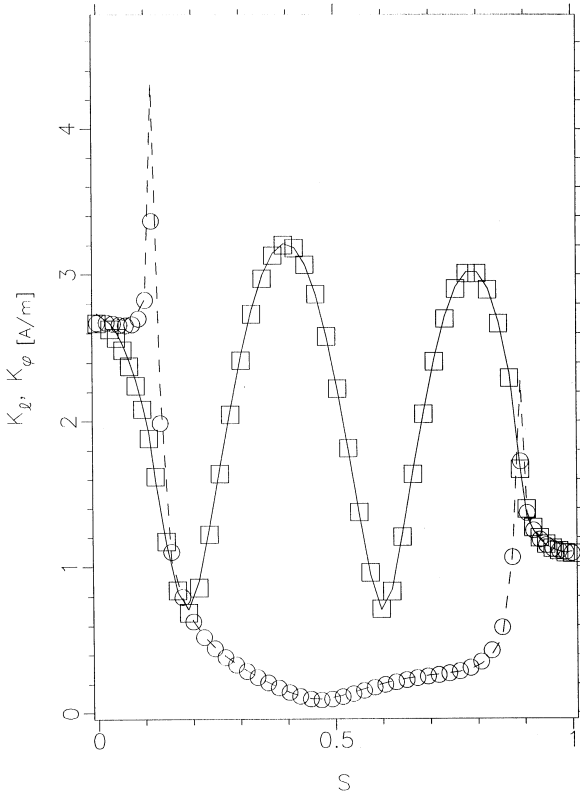


Figure 5. Magnitude of currents on a metallic pillbox above an air-earth interface with the parameters: $f = 0.3$ GHz, $\epsilon_r = 10.0$, $\sigma = 0.0$ [mho/m], $\theta^i = 0.0^\circ$, $a = 0.159\lambda_o$, $L = 1\lambda_o$ and $d = 0.1\lambda_o$. EFIE-BOR: K_ℓ —, K_ϕ - - -. MFIE-BOR: K_ℓ □□□, K_ϕ ○○○.

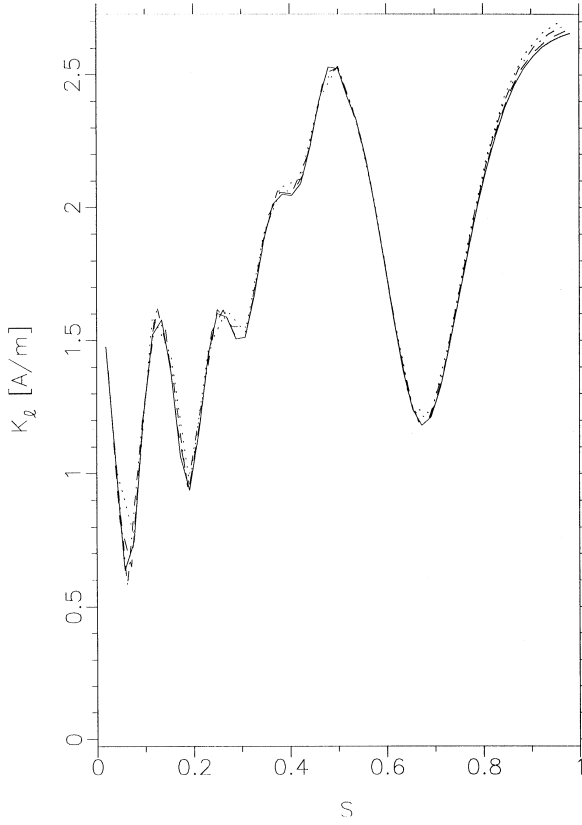


Figure 6. Magnitude of K_ℓ using MFIE-BOR on a half-buried metallic sphere with the parameters: $\epsilon_1 = 10.0$, $\epsilon_2 = 1.0$, $\theta^i = 0.0^\circ$, $a = 0.4\lambda_o$. NS = 25 : $\cdots\cdots$, NS = 31 : $-\cdot-$, NS = 41 : $---$, NS = 51 : $---$.

the modal Sommerfeld integrals which arise in the formulation. A comparison with the EFIE-BOR formulation from the convergence point of view is addressed. The CPU time for generating the equivalent matrix of EFIE/MFIE is multiples of its corresponding free space case. This means that the saving in CPU time using MFIE is more pronounced in layered media compared with free space. A case study of a sphere in contiguous half-spaces has shown a considerable saving in CPU time using MFIE. This makes MFIE more advantageous than EFIE for the analysis of a closed object in layered media.

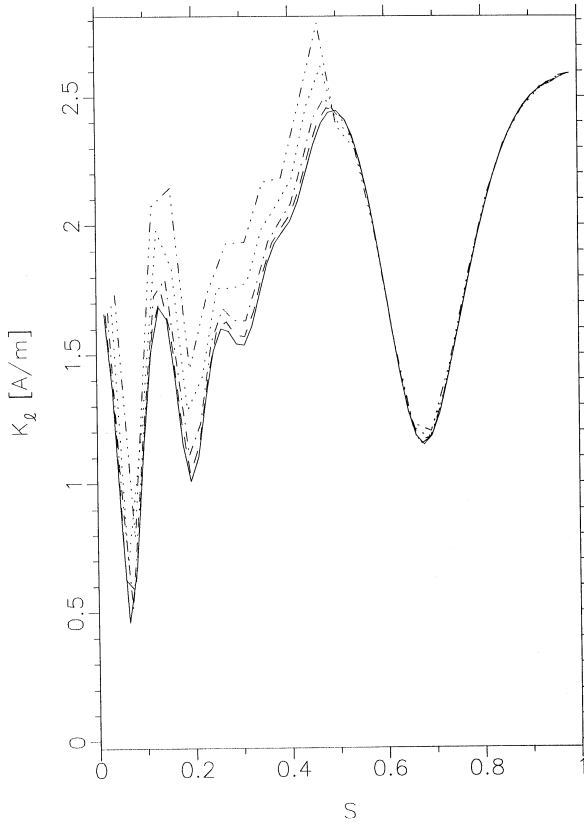


Figure 7. Magnitude of K_ℓ using EFIE-BOR on a half-buried metallic sphere with the parameters: $\epsilon_1 = 10.0$, $\epsilon_2 = 1.0$, $\theta^i = 0.0^\circ$, $a = 0.4\lambda_0$. NS = 25 : - · - · - ·, NS = 31 : ·····, NS = 41 : - · - ·, NS = 51 : - - -, NS = 61 : —.

REFERENCES

1. Abdelmageed, A. K., K. A. Michalski, and A. W. Glisson, "Analysis of EM scattering by conducting bodies of revolution in layered media using the discrete complex image method," in *Digest IEEE AP-S Int. Symp.*, 402–405, Newport, Ca, 1995.
2. Poggio, A. J. and E. K. Miller, "Integral equation solutions of three-dimensional scattering problems," in *Computer Techniques for Electromagnetics*, R. Mittra (Ed.), 129–163, Pergamon Press, New York, 1973.

3. Mohsen, A., "On the evaluation of Sommerfeld integrals," *IEE Proc., Pt. H*, Vol. 129, 177–182, 1982.
4. Fang, D. G., J. J. Yang, and G. Y. Delisle, "Discrete image theory for horizontal electric dipoles in a multilayered medium," *IEE Proc., Pt. H*, Vol. 135, 297–303, 1988.
5. Hua, Y. and T. K. Sarkar, "Generalized pencil-of-function method for extracting poles of an EM system from its transient response," *IEEE Trans. Antennas Propagat.*, Vol. 37, 229–234, 1989.
6. Harrington, R. F., *Time-Harmonic Electromagnetic Fields*, McGraw-Hill, New York, 1961.
7. Michalski, K. A. and D. Zheng, "Electromagnetic scattering and radiation by surfaces of arbitrary shape in layered media, Part I: Theory," *IEEE Trans. Antennas Propagat.*, Vol. 38, 335–344, 1990.
8. Michalski, K. A. and D. Zheng, "Electromagnetic scattering and radiation by surfaces of arbitrary shape in layered media, Part II: Implementation and results for contiguous half-spaces," *IEEE Trans. Antennas Propagat.*, Vol. 38, 345–352, 1990.
9. Abramowitz, M. and I. Stegun (Eds.), *Handbook of Mathematical functions*, Dover, New York, 1970.
10. Chew, W. C., *Waves and Fields in Inhomogeneous Media*, Ch. 2, Van Nostrand Reinhold, New York, 1990.
11. Glisson, A. W. and D. R. Wilton, "Simple and efficient numerical methods for problems of electromagnetic radiation and scattering from surfaces," *IEEE Trans. Antennas Propagat.*, Vol. 28, 593–603, 1980.